

Sequential Graph Convolutional Network for Active Learning

Razvan Caramalau Binod Bhattarai Tae-Kyun Kim

Department of Electrical and Electronics Engineering, Imperial College London, UK
 {r.caramalau18, b.bhattarai, tk.kim}@imperial.ac.uk

Abstract

We propose a novel generic sequential Graph Convolution Network (GCN) training for Active Learning. Each of the unlabelled and labelled examples is represented through a pre-trained learner as nodes of a graph and their similarities as edges. With the available few labelled examples as seed annotations, the parameters of the Graphs are optimised to minimise the binary cross-entropy loss to identify labelled vs unlabelled. Based on the confidence score of the nodes in the graph we sub-sample unlabelled examples to annotate where inherited uncertainties correlate. With the newly annotated examples along with the existing ones, the parameters of the graph are optimised to minimise the modified objective. We evaluated our method on four publicly available image classification benchmarks. Our method outperforms several competitive baselines and existing arts. The implementations of this paper can be found here: <https://github.com/razvancaramalau/Sequential-GCN-for-Active-Learning>

1 Introduction

Deep learning has shown great advancements in computer vision [1, 2] with the cost of large-scale annotated data sets. Data annotation is time-consuming, needs experts and is expensive. There are numerous fields such as medical imaging where data annotation is even more challenging. Moreover, while optimizing deep neural network architectures a gap is present concerning the representatives of the data. To overcome these issues, *active learning* [3, 4] has been successfully deployed to efficiently select the most meaningful samples. In this paper, we propose a novel generic sequential Graph Convolutional Network (GCN) for Active Learning. Majority of the previous works [5, 3, 6, 7, 8, 9, 10] integrate both the selection method and the learner together. This restricts the model to a specific type of task. Unlike these works, our model trains both the learner and sampling methodology separately, making it task agnostic similar to [11, 12].

Graph Convolutional Networks [13, 14] are a powerful tool to induce higher-order representations of nodes by performing message passing operations between the neighbouring nodes. Our objective is to exploit such strength of GCN to discard redundant unlabelled samples for effective labelling. To this end, we represent all the available data in the form of a graph. Each node encodes image description and the edges give an idea of the similarities. In the beginning, we randomly select a few examples to annotate. These labelled examples act as seeds to propagate the labelled data information to the neighbouring nodes and identify look-a-like unlabelled examples. Then, we learn the parameters of the Graph to minimise the binary-cross entropy to identify the labelled and unlabelled examples. We sort the examples based on the confidence scores through an uncertainty sampling approach and apply to sub-sample the examples to annotate. We flip the labels of the latest annotated examples from unlabelled to labelled and train the Graph to minimise the modified objective. This enables us to identify the unlabelled data manifolds which are redundant to the labelled examples. Recently, VAAL [11] trained a variational auto-encoder (VAE) [15] in an adversarial manner to map images

to a latent space where labelled vs unlabelled examples better discriminate. However, this method ignores the neighbouring relations between the examples and also there is no such mechanism for message passing. Furthermore, we gather the node information and distribute it as in CoreSet [16] for a new sampling technique. CoreSet [16] uses risk minimisation between core-sets over the learner feature space while ours uses the GCN representations. Thus, it also does not propagate the information between the data.

We evaluated our sampling methods on four challenging benchmarks and compared with several baselines and existing arts including CoreSet and VAAL. From both quantitative and qualitative comparisons, our method is more accurate and efficient than existing arts.

2 Related work

Uncertainty-based methods. Earlier techniques for sampling unlabelled data have been explored through uncertainty exploration of the CNN. A Bayesian approximation introduced in [17] produce meaningful uncertainty measurements by variational inference of a Monte Carlo Dropout (MC Dropout) adapted architecture. Hence, it is successfully integrated in active learning by [3, 18, 19, 20]. With the rise of GPU computation power, [6] ensembled classical techniques and outperformed MC uncertainty-based Dropout.

Geometric-based methods Although there have been studies exploring the data space through the representations of the learning model ([4, 21, 22]), the first work applying it for CNNs as an active learning problem has been presented in [16]. Their key principle relies on minimising the difference between the loss of labelled set and a small subset through a geometric-defined bound.

Model-based methods. Recently, a new category has been approached in the active learning methodology where separate models than learner are trained for finding meaningful data. Our method is based on this category. One of the first approaches [12] attached a loss-learning module so that loss can be predicted offline for the unlabelled samples. In [11], another task-agnostic solution deploys a variational auto-encoder (VAE) to map the available data on a latent space. They train a discriminator in an adversarial manner to classify labelled from unlabelled. The advantage of our method over this approach is exploitation of relative relationship between the examples and also sharing information between the examples enabled by message passing operations in GCN.

GCNs in active learning. GCN [13] has successfully been applied in [7, 8, 9, 10] for active learning. In comparison to these methods, our approach has distinguished learner and sampler. It makes our approach task-agnostic and also gets benefited from model-based methods mentioned just before. Moreover, none of these methods are trained in an sequential manner. However, all of them integrated the selection mechanism on the GCN learner. Thus, their active learning framework remains dependent on the graph architecture. [8] proposes K-Medoids clustering for the feature propagation between the labelled and unlabelled nodes. A regional uncertainty algorithm is presented in [7] by extending the PageRank [23] algorithm to the active learning problem. Similarly, [24] applies GCN few-shot active learning while our method is designed for supervised learning algorithms.

3 Methodology

In this section, we describe the proposed methodology in details. Given plenty of unlabelled data, at a high-level, the active learning framework has three major components: a learning algorithm, a labelling oracle and a sampling/selection mechanism. The main goal of this process is to find the most representative samples so that in a limited budget of data the highest performance is yielded. First, we briefly present the learner for the image classification task under the pool-based active learning scenario. Then, in the second part where our contribution lies, we propose a novel sequential GCN selection mechanism with two adapted sampling techniques: CoreSet [16] and uncertainty sampling [25]. We define those query methods as **CoreGCN**, the geometric approach inspired from [16], and he uncertainty-based as **UncertainGCN**. A visual description of our proposed pipeline is illustrated in Figure 1.

3.1 Learner

In our application, the learner acts as an image classifier where C classes are identified. We deploy a deep CNN model \mathcal{M} , *ResNet-18*[1] or *VGG-11*[26], that maps a set of inputs $\mathbf{x} \in \mathbf{X}$ to a

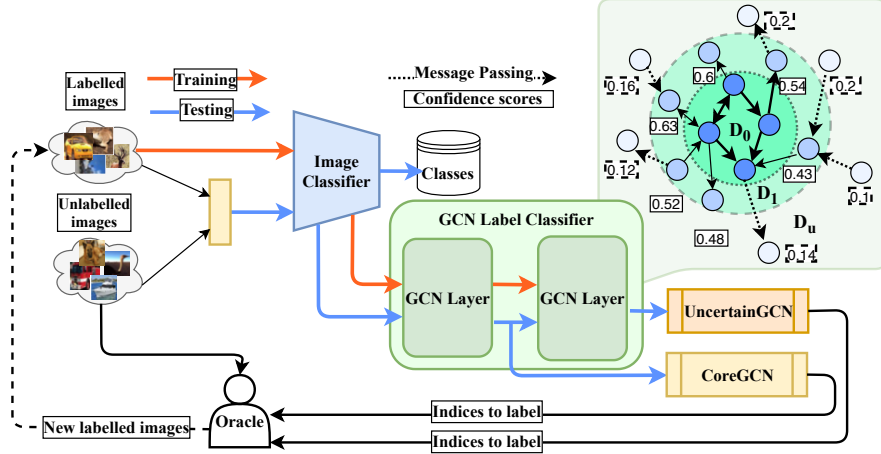


Figure 1: Schematic diagram showing the proposed pipeline. Here, *Image classifier* depicts our learner and *GCN* block represents the selection framework which are the key components of active learning pipeline.

discriminatory space of outputs $\mathbf{y} \in \mathbf{Y}$ with parameters θ . However, any other type of discriminative model can be deployed. A loss function $\mathcal{L}(\mathbf{x}, \mathbf{y}; \theta)$ is minimized during the training process. The objective function of our classifier is cross-entropy defined as below:

$$\mathcal{L}_{\mathcal{M}}(\mathbf{x}, \mathbf{y}; \theta) = -\frac{1}{N_l} \sum_{i=1}^{N_l} \mathbf{y}_i \log(f(\mathbf{x}_i, \mathbf{y}_i; \theta)), \quad (1)$$

where N_l is the number of labelled training examples and $f(\mathbf{x}_i, \mathbf{y}_i; \theta)$ is the posterior probability of the model \mathcal{M} .

Suitable for deep learning models which require sets of data, we create the framework in a pool-based scenario. Therefore, we consider an unlabeled dataset \mathbf{D}_U from which we randomly select an initial batch for labelling $\mathbf{D}_0 \subset \mathbf{D}_U$. In the active learning research, the aim is to identify with which acquisition function \mathcal{A} minimum loss can be achieved with less amount of batches \mathbf{D}_n . This scope can be simply defined for n number of active learning stages as following:

$$\min_n \min_{\mathcal{L}_{\mathcal{M}}} \mathcal{A}(\mathcal{L}_{\mathcal{M}}(\mathbf{x}, \mathbf{y}; \theta) | \mathbf{D}_0 \subset \dots \subset \mathbf{D}_n \subset \mathbf{D}_U). \quad (2)$$

We want to minimise the number of stages so that fewer samples (\mathbf{x}, \mathbf{y}) would require annotation. For the acquisition function \mathcal{A} , we want to bring the heuristic relation between the discriminative understanding of the model and the unlabelled data space. This would be traced through the performance of the algorithm at each query stage.

3.2 Sequential GCN selection process

During sampling, our contribution relies on sequentially training a GCN with the features generated from the pre-trained learner for both labelled and unlabelled images at every active learning stage. Similar to VAAL [11], we consider this methodology as model-based where another architecture is required for sampling. Our motivation in introducing the graph is primarily formed in propagating the inherited uncertainty within the feature space of the learner. Thus, message passing between the nodes brings more informativeness by inducing higher-order latent representation. Finally, our GCN will act as a binary classifier deciding which images are annotated.

3.2.1 Graph Convolutional Network

The key parts of the graph architecture \mathcal{G} are the nodes \mathcal{V} and the edges \mathcal{E} through which message passing happens according to an adjacency matrix A . The nodes $\mathbf{v} \in \mathbb{R}^{m \times N}$ of the graph are the

outputs of the feature extractor from both N labelled and unlabelled data (m represents the feature dimension of each node). Once we apply l_2 normalisation to the input features, the initial elements of A result as vector product between each sample \mathbf{v} ($S_{ij} = \mathbf{v}_i^\top \mathbf{v}_j$). Furthermore, we subtract from it the identity matrix I and then we normalise by multiplying with its degree D . Finally, we add the self-connections back so that the closest correlation is with the node itself. This can simply be summarised under:

$$A = D^{-1}(S - I) + I. \quad (3)$$

To avoid smoothness or similarity between features in deep GCN [13], we design a two-layer architecture. The first GCN layer can be described as a function $f_G^1(A, \mathcal{V}; \Theta_1) : \mathbb{R}^{N \times N} \times \mathbb{R}^{m \times N} \rightarrow \mathbb{R}^{h \times N}$ where h is number of hidden units and Θ_1 are its parameters. A rectified linear unit activation [27] is applied after the first layer to maximise feature contribution. However, to map the nodes as labelled or unlabelled, the final layer is activated through sigmoid. Thus, The output of f_G is a vector length of N with values between 0 and 1 (where 0 is considered unlabelled and 1 is for labelled). We can further define the entire network function as:

$$f_G = \sigma(\Theta_2(\text{ReLU}(\Theta_1 A)A)). \quad (4)$$

In order to satisfy this objective, our loss function will be defined as:

$$\mathcal{L}_G(\mathcal{V}, A; \Theta_1, \Theta_2) = -\frac{1}{N_l} \sum_{i=1}^{N_l} \log(f_G(\mathcal{V}, A; \Theta_1, \Theta_2)_i) - \frac{\lambda}{N - N_l} \sum_{i=N_l+1}^N \log(1 - f_G(\mathcal{V}, A; \Theta_1, \Theta_2)_i), \quad (5)$$

where λ acts as a bias between the labelled and unlabelled cross-entropy.

3.2.2 Uncertainty sampling for GCN

Once the training of the GCN is complete, we move forward to the sampling stage. From the remaining unlabelled samples \mathbf{D}_U , we can draw their confidence scores $f_G(\mathbf{v}_i; \mathbf{D}_U)$ as outputs of the GCN. Similarly to uncertainty sampling, we propose to select with our method, **UncertainGCN**, the unlabelled images with the confidence around a variable s_{margin} . While querying a fixed number of b points for a new subset \mathbf{D}_L , we apply the following equation:

$$\mathbf{D}_L = \mathbf{D}_L \cup \arg \max_{i=1 \dots b} (s_{margin} - f_G(\mathbf{v}_i; \mathbf{D}_U)). \quad (6)$$

This stage is repeated as long as equation 2 is satisfied. In the experiment section, we will also analyse the choice for s_{margin} . Algorithm 1 summarises the GCN sequential training with the UncertainGCN sampling method.

Algorithm 1 UncertainGCN active learning algorithm

```

1: Given: Initial labelled set  $\mathbf{D}_0$ , unlabelled set  $\mathbf{D}_U$  and query budget  $b$ 
2: Initialise  $(\mathbf{x}_L, \mathbf{y}_L)$ ,  $(\mathbf{x}_U)$  - labelled and unlabelled images
3: repeat
4:    $\theta \leftarrow f(\mathbf{x}_L, \mathbf{y}_L)$  ▷ Train learner with labelled
5:    $\mathcal{V} = [\mathbf{v}_L, \mathbf{v}_U] \leftarrow f(\mathbf{x}_L \cup \mathbf{x}_U; \theta)$  ▷ Extract features for labelled and unlabelled
6:   Compute adjacency matrix  $A$  according to Equation 3
7:    $\Theta \leftarrow f_G(\mathcal{V}, A)$  ▷ Train the GCN
8:   for  $i = 1 \rightarrow b$  do
9:      $\mathbf{D}_L = \mathbf{D}_L \cup \arg \max_i (s_{margin} - f_G(\mathbf{v}; \mathbf{D}_U))$  ▷ Add nodes depending on the label
     confidence
10:  end for
11:  Label  $\mathbf{y}_U$  given new  $\mathbf{D}_L$ 
12: until Equation 2 is satisfied

```

3.2.3 CoreSet sampling for GCN

In order to integrate geometric information between the labelled and unlabelled graph representation, we approach a CoreSet technique [16] in our sampling stage. This has shown better performance

in comparison to uncertainty-based methods [8]. In [16], they show how bounding the difference between the loss of the unlabelled samples and the one of the labelled is similar to the k -Centre minimisation problem stated in [28].

In their approach, they sample based on the l_2 distances between the features extracted from the trained classifier. Instead of that, we will make use of our GCN architecture by applying their method on the features represented after the first layer of the graph. Their sampling method is adapted to our mechanism for each b data point under equation:

$$\mathbf{D}_L = \mathbf{D}_L \cup \arg \max_{i \in \mathbf{D}_U} \min_{j \in \mathbf{D}_L} \delta(f_G^1(A, \mathbf{v}_i; \Theta_1), f_G^1(A, \mathbf{v}_j; \Theta_1)), \quad (7)$$

where δ is the Euclidean distance between the graph features of the labelled node \mathbf{v}_i and the ones from the unlabelled node \mathbf{v}_j . We define this method as **CoreGCN**.

Finally, given the model-based mechanism, we claim that our acquisition functions are task-agnostic as long as the learner is producing a form of feature representations. In the following section, we will experimentally demonstrate the performance of our method quantitatively and qualitatively.

4 Experiments

Implementation details: As mentioned, we have two separate components in our pipeline: learner and sampler (acquisition function). For the learner, we chose ResNet-18 [1] due to its high accuracy and better training stability in comparison to other contemporary architectures. During training, as shown in Equation 1, we minimize cross-entropy loss over a fixed 128 batch size. We optimise with Stochastic Gradient Descent (SGD) keeping a weight decay at 5×10^{-4} and momentum at 0.9. At every selection stage, we train the model in 200 epochs starting with a learning rate of 0.1 and decreasing it to 0.01 after 160 epochs. We keep these hyper-parameters same throughout all experiments. Similarly, our acquisition function (sampler) is approximated by the GCN with trained in a sequential manner. We choose 2 layers of GCN and set dropout to 0.3 to avoid over smoothing [29]. The objective function is binary cross-entropy per node with the bias λ between labelled and unlabelled samples. We set the value of $\lambda = 1.2$ to give more importance to unlabelled points. For optimisation, we chose Adam [30] with a weight decay of 5×10^{-4} and a learning rate of 10^{-3} . The nodes of the graphs are initialised with the features of the images extracted from the learner network’s latest model parameters. And these features are projected to the dimension of 128. Such initialisation connects the learner with the acquisition function (sampler). We performed ablation studies to select these hyper-parameters which we present shortly. In the uncertainty-based sampling method, according to equation 6, we have the s_{margin} variable to set. From our ablation studies, we observed that our method selects the most informative samples when s_{margin} equals 0.1.

Compared methods: We compare the performance of our selection mechanism against following three comparable and state-of-the-art techniques.

Random: For each subset, we uniformly sample b points from the entire unlabelled data set. This is the most common practice.

CoreSet[16]: The purpose of this method is to find b unlabelled samples that will act as new centres while the now reduced radius will cover the entire feature space.

VAAL[11]: We consider this work as one of the closest to our work. This method trains VAE with both labelled and unlabelled samples to learn a discriminative subspace in an adversarial manner.

Learning Loss[12]: This method is state-of-the-art method to date. This method proposes to minimise learning loss as an additional loss in the learner.

Datasets and experiment settings We evaluated our method together with the others on four challenging image classification benchmarks: CIFAR-10[31], CIFAR-100[31], FashionMNIST[32] and SVHN[33]. Each of the datasets has different properties and present new challenges for the active learning framework. CIFAR-10 consists of 50,000 images for training and 10,000 for testing. There are 5,000 samples for each of the 10 object categories. CIFAR-100 is constructed in a similar fashion with the same size of the training and testing set. The difference is in the granularity of the data distribution as 100 classes are categorised (500 images corresponding to each class). The SVHN dataset represents 10 digit classes in 73,257 train images and 26,032 test images. Finally, FashionMNIST contains training and testing sets of the size 60,000 and 10,000, respectively, with annotations of 10 clothing designs.

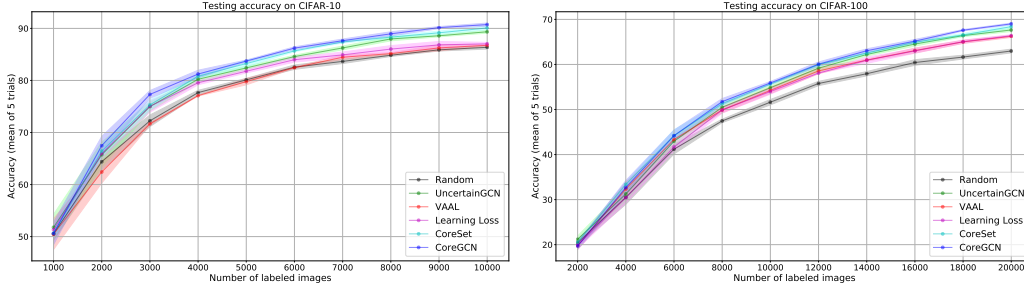


Figure 2: Quantitative comparison on CIFAR-10(left) and CIFAR-100(right) (Zoom in the view)

For every dataset, we assume that all training images are unlabelled (\mathbf{D}_U) in the beginning. The initial labelled set \mathbf{D}_L will be formed of 1,000 random sampled images for the CIFAR-10, SVHN and FashionMNIST experiments. Because of the fine-grained structure of CIFAR-100, during the first active learning stage, 2,000 will be selected for labelling. We will conduct our experiments along 10 stages, while at every stage the same number of queries will be produced by the proposed acquisition functions (1,000 b points for the 10-class datasets and 2,000 for CIFAR-100). Similarly to the works in [6, 12], before selection, we will create randomly a subset $\mathbf{D}_S \subset \mathbf{D}_U$ from the unlabelled images to avoid the redundancy occurrence common to those datasets. The \mathbf{D}_S size will be 10,000 for all the active learning stages in every experiment.

Evaluation Metrics: We report the mean average accuracy of the 5 trials on test sets for every dataset.

Quantitative Comparisons Firstly, we evaluated ResNet-18 for all the benchmarks on their entire data. We obtain for CIFAR-10 and CIFAR-100 a classification rate of 93.09% and 73.02%, respectively. For the other two data sets, our learner yielded 93.74% on FashionMNIST, whereas on SVHN we obtain 95.35%.

Figure 2 (left) shows the performance of UncertainGCN and CoreGCN against the other four existing arts on CIFAR-10 dataset under the specified experiment settings. The solid line of the representation is the mean averaged accuracy, while the faded colour shows the standard deviation after the 5 trials. Our GCN-based mechanism with the two sampling techniques surpasses random sampling and VAAL at every selection stage by at least 4%. After 10,000 labelled examples, the CoreGCN achieves state-of-the-art with 90.7%, the highest reported value in the literature [12, 11] under this configuration. The performance obtained with a fifth of \mathbf{D}_U brings an important factor to the research community in whether labelling 40,000 more images is needed for a 2.4% gain. UncertainGCN comes close to CoreSet achievements over the testing set, but it is limiting in latter stages due to the selection from confused feature-space areas. This aspect is demonstrated in the qualitative analysis.

Following the quantitative study on CIFAR-100 Figure 2 (right), we indicate that our proposed methods can scale to a more diverse dataset maintaining their state-of-the-art results. With 40% of labelled data, we achieve 69% accuracy by applying CoreGCN (4% less than from the entire dataset). Once again, the GCN capacity of passing information within the feature domain helps furthermore the active learning sampling. Compared to CIFAR-10, VAAL shows a better trend against random sampling, but it still falls under our performances. The reason is that the VAE might require a larger batch of queries (1,000 more) to differentiate. On the other side, although Learning Loss outperforms VAAL on the other datasets, for CIFAR-100 the mean averaged performance is similar.

We continue the image classification analysis on FashionMNIST and SVHN by illustrating performance progressions in Figure 3. The challenge in those datasets consists in the high accuracy already obtained from the initial random set \mathbf{D}_0 . This happens due to the ResNet-18’s discriminatory capability and because of the saturation within the data space. In the FashionMNIST experiment, apart from VAAL and Learning Loss, all of our selection methods follow similar curves over-passing random at every query stage. We show that there are no obvious differences between the UncertainGCN and CoreGCN performances for greyscale data, especially with low-complexity features. We notice the same behaviour for the SVHN dataset. The mean averaged accuracy plateaus after 6,000 labelled points around 92.5% for CoreGCN, while CoreSet and UncertainGCN follow up in the next stages.

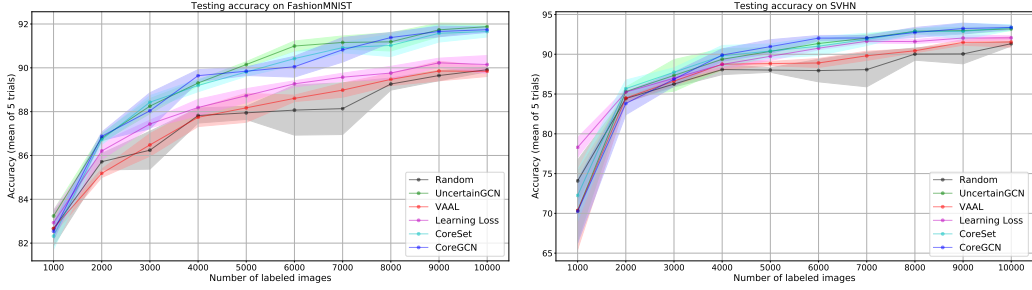


Figure 3: Quantitative comparison on FashionMNIST(left) and SVHN(right) (Zoom in the view)

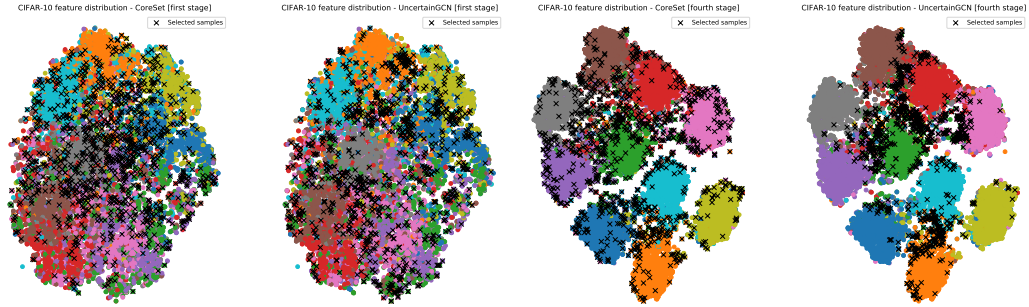


Figure 4: Exploration comparison on CIFAR-10

In this set of experiments, we observe that our GCN selection approach exceeds in terms of mean averaged accuracy in comparison to existing model-based methods like VAAL and Learning Loss. Overall comparisons demonstrate the clear superior performance of the proposed method compared to the recent arts in active learning.

Qualitative Comparisons We assume that ideally, the selection method aims to uniformly sample from all the classes at the initial annotation stages. Once the learner becomes more confident, the acquisition function should explore more samples from uncertain areas. Because in our active learning framework the exploitation factor is fixed to either 1,000 or 2,000, we will observe the exploration aspect through t-SNE [34] representations.

We compute embedding of the ResNet-18 CIFAR-10 features from both labelled and unlabelled samples for the first and fourth query stage. In Figure 4, the t-SNE algorithms clusters the images of the 10 categories for both CoreSet and UncertainGCN. From an exploration perspective, UncertainGCN targets out-of-distribution samples and areas where features are hardly distinguished. We select nodes with label confidence values around $s_{margin} = 0.1$. The reason is to select the most confident unlabelled samples that are found closer to 0. Furthermore, the uncertainty is inherited by the GCN binary classifier through its inability to correlate the multi-class nodes to the annotation information. As mentioned in the quantitative part, Figure 4(right) shows the concentrated uncertain areas of this method. Since at first stages the features are concentric, the GCN will sparsely spread the messages between the nodes. When the CoreSet is applied on the graph, the bound over the core-set loss (defined in [16]) is extended through the new feature space.

Ablation studies In this part, we investigate what is the impact of the GCN hyper-parameters and its uncertainty-based selection variables on the performance. Furthermore, given the current active learning framework, we observe the effect using different features by changing the learner’s architecture from ResNet-18 to VGG-11 [26].

While varying the architectural parameters of the GCN binary classifier, we encountered a poorer selection with the increase of the Dropout rate from 0.3 to 0.5 or 0.8. However, when changing the

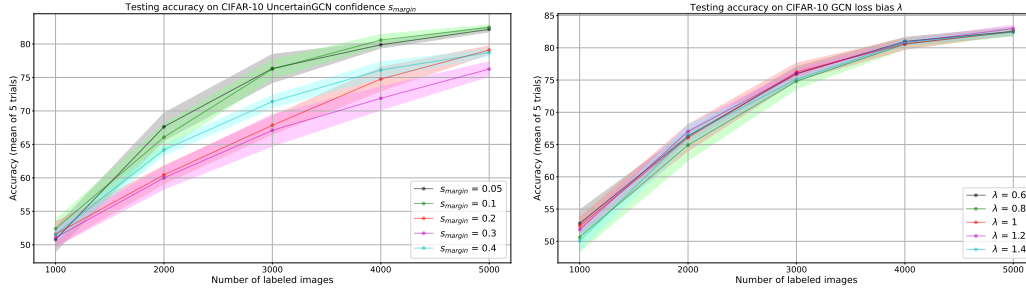


Figure 5: UncertainGCN tuning parameters (Zoom in the view)

Table 1: Learner comparison [Resnet-18 vs VGG-11] - 4,000 CIFAR-10 labelled images [mean averaged accuracy on 5 trials]

	Random	VAAL	CoreSet	Learn. Loss	UncertainGCN	CoreGCN
ResNet-18[1]	77.66	77.48	80.81	80.25	80.22	81.23
VGG-11[26]	70.9	69.98	68.54	68.13	72.35	71.32

size of the hidden units to 256 and 512, the UncertainGCN sampling was not affected on CIFAR-10. This might require further optimisation for different datasets.

The main principle in UncertainGCN is focused on uncertainty sampling. In section 3.2, we defined the parameter s_{margin} to tune according to the GCN binary classification. Figure 5 (left) suggests that least confident samples (closer to 0.5) are not representative to the testing set. Another key parameter in both UncertainGCN and CoreGCN query functions is λ , the loss bias between the labelled and unlabelled data points. We observe in Figure 5 (right) that the mean averaged accuracy on CIFAR-10 slightly improves in first stages when the bias is shifted to the unlabelled loss by 20%.

In Table 1, we modified the architecture of the learner for CIFAR-10 experiment to VGG-11 for analysing how the acquisition functions are affected in terms of accuracy at the fourth sampling stage. In training the VGG-11 network, we kept the same hyper-parameters. We also had to trace the features after the first four Max Pooling layers for the Learning Loss baseline. Our proposed methods present robustness to this change, however settings were left unchanged. Hence, they surpass all state-of-the-arts at this early stage. This also demonstrates how the batch size and the feature representation play an important role in the performances of the other baselines.

In terms of efficiency, we evaluated the number of the parameters of VAAL and Learning Loss in comparison to ours as they fall within the same active learning category. For selecting samples with VAAL a variational auto-encoder and a discriminator need to be trained in an adversarial manner. Thus, the total number of parameters for their proposed architecture is 23,115,204. Although they claim efficient sampling speed, our GCN sampling technique requires only 82,307. Moreover, this quantity even falls shorter than the Learning Loss module which has 123,905 parameters. This proves that our method is the fastest of all the model-based acquisition functions.

5 Conclusion and future work

We have presented a novel methodology of active learning in image classification using Graph Convolutional Network. After systematical and comprehensive experiments, our adapted sampling techniques, UncertainGCN and CoreGCN, produced state-of-the-art results on four benchmarks. We have shown through qualitative distributions that our selection functions maximises informativeness within the data space. The design of our sampling mechanism allows being integrated into other learning tasks. Furthermore, this approach enables further investigation in this direction where both uncertain and geometric methods could be combined.

Acknowledgements

This work is partially supported by Huawei Technologies Co. and by EPSRC Programme Grant FACER2VM (EP/N007743/1).

References

- [1] Kaiming He, Xiangyu Zhang, Shaoqing Ren, and Jian Sun. Deep residual learning for image recognition. In *CVPR*, pages 770–778, 2016.
- [2] Alex Krizhevsky, Ilya Sutskever, and Geoffrey E Hinton. Imagenet classification with deep convolutional neural networks. In *NIPS*, 2012.
- [3] Yarin Gal, Riashat Islam, and Zoubin Ghahramani. Deep Bayesian Active Learning with Image Data. In *ICML*, 2017.
- [4] Aryeh Kontorovich, Sivan Sabato, and Ruth Uner. Active nearest-neighbor learning in metric spaces. In *NeurIPS*, 2016.
- [5] Corinna Cortes and Vladimir Vapnik. Support-vector networks. *Machine learning*, 20(3):273–297, 1995.
- [6] William H Beluch Bcai, Andreas Nürnberger, and Jan M Köhler Bcai. The power of ensembles for active learning in image classification. In *CVPR*, 2018.
- [7] Roy Abel and Yoram Louzoun. Regional based query in graph active learning, 2019. 1906.08541v1.
- [8] Yuexin Wu, Yichong Xu, Aarti Singh, Yiming Yang, and Artur Dubrawski. Active Learning for Graph Neural Networks via Node Feature Propagation, 2019. 1910.07567v1.
- [9] Hongyun Cai, Vincent W Zheng, and Kevin Chen-Chuan Chang. Active Learning for Graph Embedding, 2017. 1705.05085v1.
- [10] Li Gao, Hong Yang, Chuan Zhou, Jia Wu, Shirui Pan, and Yue Hu. Active discriminative network representation learning. In *IJCAI*, pages 2142–2148, 2018.
- [11] Samarth Sinha, Sayna Ebrahimi, and Trevor Darrell. Variational Adversarial Active Learning. In *ICCV*, 2019.
- [12] Donggeun Yoo and In So Kweon. Learning Loss for Active Learning. In *CVPR*, 2019.
- [13] Thomas N Kipf and Max Welling. Semi-supervised classification with graph convolutional networks. In *ICLR*, 2017.
- [14] Michael M Bronstein, Joan Bruna, Yann LeCun, Arthur Szlam, and Pierre Vandergheynst. Geometric deep learning: going beyond euclidean data. *IEEE Signal Processing Magazine*, pages 18–42, 2017.
- [15] Yunchen Pu, Zhe Gan, Ricardo Henao, Xin Yuan, Chunyuan Li, Andrew Stevens, and Lawrence Carin. Variational autoencoder for deep learning of images, labels and captions. In *NeurIPS*, 2016.
- [16] Ozan Sener and Silvio Savarese. Active Learning for Convolutional Neural Networks: A Core-set approach. In *ICLR*, 2018.
- [17] Yarin Gal and Zoubin Ghahramani. Dropout as a Bayesian Approximation: Representing Model Uncertainty in Deep Learning. In *ICML*, 2016.
- [18] Neil Houlsby, Ferenc Huszár, Zoubin Ghahramani, and Máté Lengyel. Bayesian Active Learning for Classification and Preference Learning, 2011. 1112.5745v1.
- [19] Andreas Kirsch, Joost Van Amersfoort, and Yarin Gal. BatchBALD: Efficient and Diverse Batch Acquisition for Deep Bayesian Active Learning. In *NeurIPS*, 2019.
- [20] Robert Pinsler, Jonathan Gordon, Eric Nalisnick, and José Miguel Hernandez-Lobato. Bayesian Batch Active Learning as Sparse Subset Approximation. In *NeurIPS*, 2019.
- [21] Ivor W. Tsang, James T. Kwok, and Pak-Ming Cheung. Core vector machines: Fast svm training on very large data sets. *J. Mach. Learn. Res.*, 6:363–392, December 2005.
- [22] Sarel Har-Peled and Akash Kushal. Smaller coresets for k-median and k-means clustering. In *SCG*, page 126–134, 2005.

- [23] Lawrence Page, Sergey Brin, Rajeev Motwani, and Terry Winograd. The pagerank citation ranking: Bringing order to the web. Technical Report 1999-66, Stanford InfoLab, November 1999. Previous number = SIDL-WP-1999-0120.
- [24] Victor Garcia and Joan Bruna. Few-shot learning with graph neural networks. In *ICLR*, 2018.
- [25] David D. Lewis and William A. Gale. A sequential algorithm for training text classifiers. In *SIGIR*, page 3–12, 1994.
- [26] Karen Simonyan and Andrew Zisserman. Very Deep Convolutional Network for Large-scale image recognition. In *ICLR*, 2015.
- [27] Vinod Nair and Geoffrey E. Hinton. Rectified linear units improve restricted boltzmann machines. In *ICML*, 2010.
- [28] Gert Wolf. Facility location: concepts, models, algorithms and case studies. In *Contributions to Management Science*, pages 331–333, 2011.
- [29] Lingxiao Zhao and Leman Akoglu. Pairnorm: Tackling oversmoothing in gnns. *ICLR*, 2020.
- [30] Diederik P Kingma and Jimmy Lei Ba. ADAM: A Method for Stochastic Optimization. In *ICLR*, 2015.
- [31] Alex Krizhevsky. Learning multiple layers of features from tiny images. *University of Toronto*, 05 2012.
- [32] Han Xiao, Kashif Rasul, and Roland Vollgraf. Fashion-MNIST: a Novel Image Dataset for Benchmarking Machine Learning Algorithms, 2017. 1708.07747v2.
- [33] Ian J Goodfellow, Yaroslav Bulatov, Julian Ibarz, Sacha Arnoud, and Vinay Shet. Multi-digit Number Recognition from Street View Imagery using Deep Convolutional Neural Networks, 2013. 1312.6082v4.
- [34] Laurens van der Maaten and Geoffrey Hinton. Visualizing data using t-sne, 2008. JMLR.

A Supplementary Material

CIFAR-10 imbalanced dataset In the experimental part, we evaluated quantitatively in a systematic manner the active learning methods over four image classification datasets. Although, before selection, we randomise the unlabelled samples to a subset, the dataset is still relatively balanced to each class distribution. However, this is not commonly the case where there is no prior information related to the data space. Therefore, we are simulating an imbalanced CIFAR-10 in a quantitative experiment. Beforehand we considered the 50,000 training set as unlabeled, given 5,000 samples for each of the 10 categories. We custom the dataset so that 5 of the 10 classes contain 10 % of their original data (500 samples each). Therefore, the new unlabelled pool is composed of 27,500 images. The experiment architecture and settings are similar to the one on the full scale.

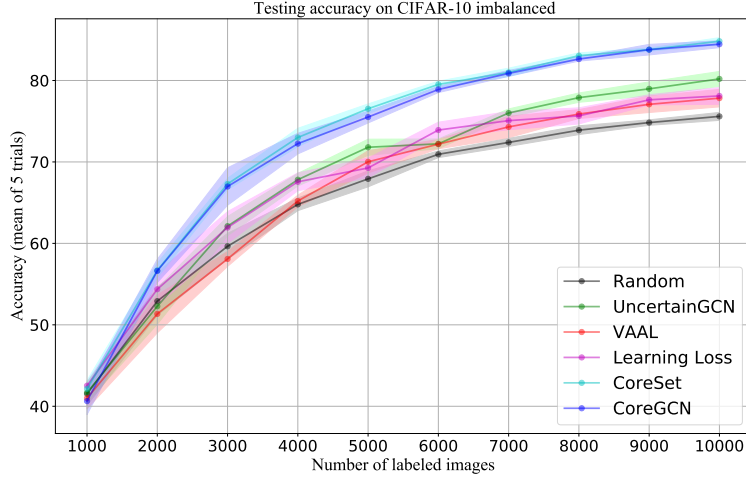


Figure A.1: Quantitative results - CIFAR-10 imbalanced dataset

Figure A.1 shows the progressions of the acquisition functions presented. Our proposed methods, UncertainGCN and CoreGCN, out-stand once again the other model-based selections like VAAL and Learning Loss. UncertainGCN scores 2% more than those methods with 80.05% mean average accuracy at 10,000 labelled samples. Meanwhile, CoreGCN achieves 84.5% top performance together with CoreSet. Thus, the geometric information is more useful in scenarios where the dataset is imbalanced.

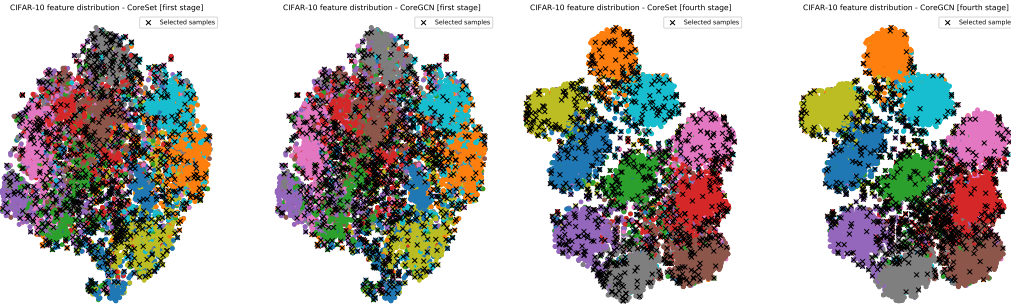


Figure A.2: Exploration comparison on CIFAR-10 between CoreSet and CoreGCN

Qualitative study extended In figure A.2, we continue the qualitative investigation for the CoreGCN acquisition method. As previously, we compare the t-SNE embeddings of the CoreGCN against CoreSet. We can observe that starting at the first selection stage, CoreGCN avoids over-populated areas while tracking out-of-distribution unlabelled data. Compared to UncertainGCN, the

geometric information from CoreGCN maintains a sparsity throughout all the acquisition stages. Consequently, it preserves the message passing through the uncertain areas while CoreSet keeps sampling closer to cluster centres. This brings a strong balance between in and out of distribution selection with the availability of more samples.

Ablation study - GCN parameter search Figure A.3.

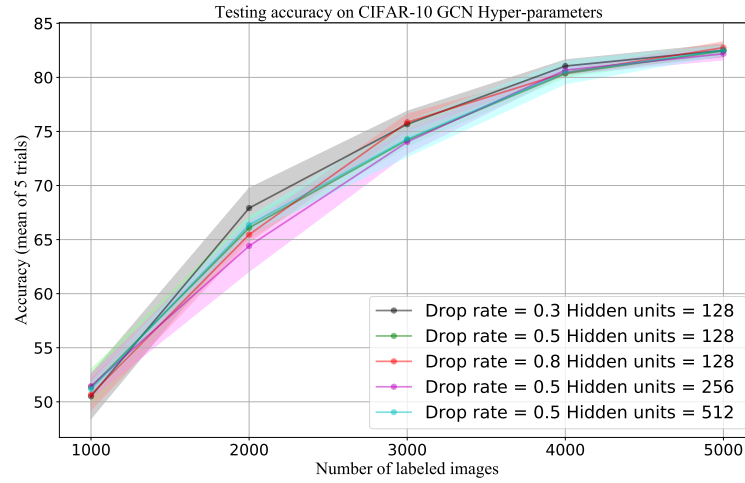


Figure A.3: Ablation studies - CIFAR-10 GCN Hyper-parameters tuning

VGG-11 learner for CIFAR-10 image classification for 3 selection stages Figure A.4.

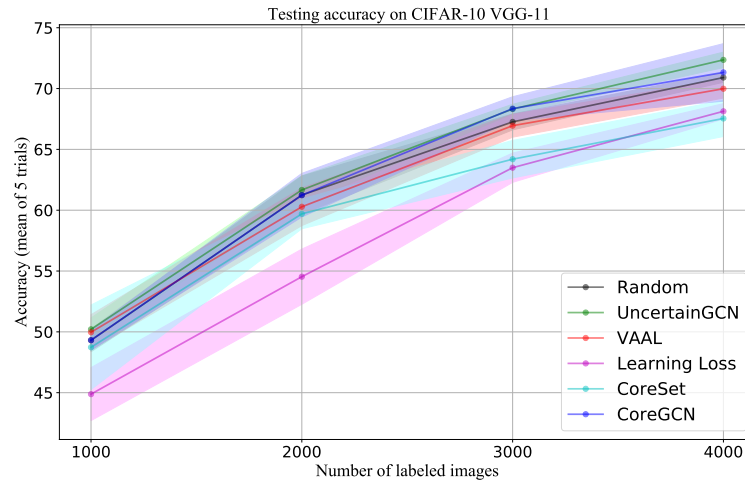


Figure A.4: CIFAR-10 Learner VGG-11 - 3 selection stages